Editors' Choice—Washing of Nickel-Rich Cathode Materials for Lithium-Ion Batteries: Towards a Mechanistic Understanding

EDITORS' CHOICE

Washing of Nickel-Rich Cathode Materials for Lithium-Ion Batteries: Towards a Mechanistic Understanding

Daniel Pritzl,[1,=,*] Tobias Teufl,[1,2,=,*,z] Anna T. S. Freiberg,[1,*] Benjamin Strehle,[1,*] Johannes Sicklinger,[1,*] Heino Sommer,[2] Pascal Hartmann,[2] and Hubert A. Gasteiger[1,]**

[1] *Chair of Technical Electrochemistry, Department of Chemistry and Catalysis Research Center, Technical University of Munich, Munich, Germany*
[2] *BASF SE, New Battery Materials and Systems, Ludwigshafen, Germany*

Washing is a commonly used method to remove surface impurities of cathode materials for lithium-ion batteries. However, a clear mechanistic understanding of the washing process is missing in the literature. In this study, we will investigate the effect of washing and subsequent drying of nickel-rich NCM cathodes (85% nickel) with respect to gassing and impedance of the washed cathodes. By on-line electrochemical mass spectrometry (OEMS), we will show a drastic reduction of the O_2 release above 80% SOC for the NCM washed with deionized water, suggesting the formation of an oxygen-depleted surface layer on the NCM particle surface. The modification of the surface can be confirmed by a strong impedance buildup of cathodes composed of washed NCM (using a micro-reference electrode in a full-cell), revealing that the impedance increases strongly with increasing drying temperature after washing. Last, we will propose a comprehensive mechanism on the processes occurring during the washing/drying process of nickel-rich NCM materials and identify the drying temperature after washing as the dominant factor influencing the surface properties.
 [DOI: 10.1149/2.1351915jes]

Manuscript submitted October 18, 2019; revised manuscript received November 8, 2019. Published December 3, 2019. This was Paper 234 presented at the Cancun, Mexico, Meeting of the Society, September 30–October 4, 2018.

Lithium-ion batteries are considered as a viable option to power electric vehicles (EVs), but several obstacles like too high battery cost and insufficient EV driving range still have to be overcome.[1,2] In principle, this can be addressed by increasing the energy density of future lithium-ion batteries, which most critically depends on the capacity of the cathode active material (CAM).[2] One of the most promising class of cathode materials to enable higher capacities are the so-called NCM and NCA materials, both having a layered structure with the sum formula $LiMeO_2$ (Me = Ni, Co, Mn for NCM, and Me = Ni, Co, Al for NCA). In current vehicles, for example, NCM-523 (Ni:Co:Mn = 5:2:3) cathodes are used,[3] showing good structural stability during lithium extraction/insertion as well as reasonable capacities of ≈160mAh/g.[3] However, higher nickel contents are required to increase the specific capacity at acceptable upper cut-off voltages, represented by nickel-rich NCMs like NCM-811 (Ni:Co:Mn = 8:1:1) or with even higher nickel content.[4] These nickel-rich NCMs can provide reversible capacities exceeding 180 mAh/g at reasonable cut-off potentials (4.2 V vs. graphite). For these nickel-rich materials manganese and aluminum can be used to stabilize the structure,[5] using aluminum leads to nickel-rich NCA, which is used by Tesla since many years.[3]

However, the increasing capacity of nickel-rich materials comes at the cost of faster capacity fading and higher sensitivity toward exposure or storage of the materials at ambient air.[6,7] It was shown that Ni-rich materials are very sensitive toward storage under humidity and CO_2 containing atmospheres,[6–9] leading to the formation of large amounts of hydroxides and carbonates on the surface of the CAM particles.[10–17] These surface impurities do not only lead to a deterioration of the capacity retention[6,8,9] and to substantial gassing during cell cycling,[8,18–21] but also lead to a high pH of the electrode coating slurries, which can cause gelation of the slurry during electrode preparation.[17,22] A simple and practical approach to remove surface contaminants taken by cell and material manufacturers is a washing step, in which the cathode active material is washed in an aqueous solution.[17,23] This washing step can significantly lower the pH value of the coating slurry[17,24] and can thus prevent gelation during the electrode coating process. Kim[25] has also shown that washing of nickel-rich cathodes can efficiently prevent gas evolution during high temperature storage experiments. It has initially been suggested that washing of NCA improves its properties by simply removing lithium carbonate and lithium hydroxide impurities from the CAM surface,[24] whereas other reports suggest also a reaction of water in the wash solution with the active material itself.[17,26]

While the removal of lithium carbonate surface impurities from NCA by washing clearly reduces the gassing upon high-temperature storage,[24,25] the effect of washing on the cycle life of Ni-rich CAMs is less clear. For example, Kim et al.[24] showed that room temperature washing of NCA followed by re-calcination at 700°C significantly improves the overall capacity and capacity retention for cycling conducted at low C-rates (0.3C) and at 25°C.[24] Similarly, Xiong et al.[26] showed that a washed NCM-811 re-calcined at 700°C also exhibits superior capacity retention compared to an unwashed material (cycling at 2C and 25°C), even though its initial capacity is slightly lower. On the other hand, Kim et al.[17] report a negative effect of washing on the cycling stability of NCA (cycling at 1C and 45°C); unfortunately, since the washing process (e.g., water/CAM ratio, temperature, etc.) and the subsequent drying/calcination temperature were not specified, it is not possible to determine whether this negative effect of washing is due to the washing/drying procedure or due to the higher cycling temperature. While one would expect that an NCM surface without any hydroxides or carbonates should perform best, some work suggests that synthesis of a material with an entirely virgin surface shows poor electrochemistry, and that a certain exposure to ambient conditions is required to create a stable surface.[11]

With regards to the structural evolution of nickel-rich CAMs, it has been shown that nickel-rich NCMs tend to form a spinel-type surface structure at high state-of-charge (SOC > 80%) induced by oxygen release,[27,28] ultimately leading to chemical electrolyte oxidation[29] and a substantial impedance build-up[27] (the same was observed for Li- and Mn-rich NCMs[30]). At the moment, many different surface stabilizations strategies are under investigation to stabilize the surface of nickel-rich layered cathode materials, such as surface sulfatation,[31,32] recalcination after exposure to the ambient,[8,9,33] as well as surface coatings with spinel structures[34] or core-shell particles.[35] Considering the results by Paulsen et al.,[11] we suggest that washing of nickel-rich materials does not only remove the well-known Li_2CO_3 and LiOH surface impurities, but also modifies the near-surface bulk properties of Ni-rich CAMs by an Li^+/H^+ ion exchange between the CAM and the wash solution,[9,36,37] which particularly in the subsequent drying/recalcination step might lead to very different near-surface structures. While washing of nickel-rich cathode materials (mostly NCA) is a well-known industrial process and is already implemented by most of

=These authors contributed equally to this work.
*Electrochemical Society Student Member.
**Electrochemical Society Fellow.
zE-mail: tobias-maximilian.teufl@basf.com

the battery manufacturers, the effect of these washing procedures and of the subsequent drying/recalcination step on the CAM properties is still not clearly understood. More detailed insights into these processes might ultimately reveal improved surface modification strategies for nickel-rich cathode active materials.

In this study we will examine the reactions that occur during the washing of the nickel-rich cathode active material $LiNi_{0.85}Co_{0.10}Mn_{0.05}O_2$ (referred to as NCM-851005) in deionized water and during the subsequent drying/heating step. Subsequently, the effect of the washing/drying procedure on the electrochemical properties will be examined. By means of on-line electrochemical mass spectrometry (OEMS) we could prove that washing/drying has a significant influence on the oxygen release and the overall gas evolution of NCM-851005 during the first charge, which can be rationalized by the formation of an oxygen deficient surface layer during the drying step. While titration analysis of the wash solution and X-ray photoelectron spectroscopy (XPS) of washed NCM-851005 shows that washing with water can remove lithium hydroxide and carbonate impurities from the surface without releasing oxygen (demonstrated by on-line mass spectrometry), we can clearly show by electrochemical impedance spectroscopy (EIS) and OEMS that the drying temperature most strongly affects the properties of the newly formed NCM-851005 surface. Its effect on the cycling stability of graphite/NCM-851005 full-cells will be discussed.

Experimental

Washing process of NCM-851005 powder.—For the washing process, 20 g of NCM-851005 (from BASF SE, Germany) were mixed with 100 mL of deionized water (18 MΩcm, Merck KGaA, Germany), and stirred with 700 rpm for 20 minutes at room temperature (referred to as "first washing"). The solution was then filtered, and the washed material was dried under vacuum for 4 hours either at 25°C (only for the freeze-dried sample) or at 65°C (all other samples). Subsequently, the once washed material was washed again (20 g CAM in 100 mL of deionized water), and the suspension was filtered again (referred to as "second washing").

In a first set of washing experiments, washing was conducted in an argon-filled glove box, and the filtered sample after the first washing step was dried under vacuum at 65°C for 4 hours. The pH values in the CAM/water slurry were measured as a function of time during the first and the second washing step. In addition, the concentrations of LiOH and Li_2CO_3 in the filtrated wash solutions after the first and second washing were determined by titration with HCl. Li_2CO_3 and LiOH could be distinguished due to the different equivalent points in the titration curve. The twice washed CAM was finally dried under vacuum at 180°C for 12 hours.

In a second set of washing experiments, the two washing steps were conducted at ambient atmosphere, drying the CAM in between the two washing steps under vacuum (Büchi oven) at 65°C for 4 hours. Parts of the twice washed CAM were then dried under vacuum for 12 hours at three different drying temperatures, namely at 80°C, 180°C, or 300°C under dynamic vacuum (Büchi oven). One batch of twice washed NCM-851005 (dried at 25°C between the two washing steps) was dried after the two washing steps at 25°C by freeze-drying, for which a vessel with the twice washed CAM was put into liquid nitrogen and dynamic vacuum was applied for 12 hours.

Electrode preparation.—Cathode electrode inks were prepared by dispersing 96 wt% of the pristine or the washed/dried NCM-851005, 2 wt% conductive carbon (Super-C65, Timcal, Switzerland), and 2 wt% polyvinylene difluoride PVDF binder (Kynar HSV 900, Arkema, France) in N-methyl-2-pyrrolidone NMP (anhydrous, Sigma-Aldrich, USA) using a planetary mixer (Thinky Corp.) for 10–15 minutes.

For OEMS measurements, the cathode inks were coated onto a porous stainless-steel mesh (SS316, aperture 26 μm, wire diameter 25 μm, The Mesh Company Ltd., UK) and then dried at 50°C in a convection oven, the freeze dried cathode coatings were dried at ≈25°C (ambient temperature) for at least 3 h. The NCM loading was ≈12 mg/cm^2, corresponding to ≈3.3 mAh/cm^2 (based on a theoretical capacity of 275 mAh/g for 100% delithiation). Cathode electrodes for OEMS experiments were punched out with a diameter of 15 mm.

For impedance and cycling measurements, the cathode inks were coated onto aluminum foil (MTI, 18 μm) with a doctor blade coater and dried afterwards at 50°C in a convection oven, the freeze dried cathode coatings were dried at ≈25°C (ambient temperature) for at least 3 h. The final NCM-851005 coating had a loading of ≈9 mg_{NCM}/cm^2, corresponding to ≈2 mAh/cm^2, based on a first charge capacity of 215 mAh/g at an upper cell cutoff voltage of 4.2 V for graphite/NCM-851005 full-cells). In this specific case, the theoretical capacity was defined by the first charge capacity in order to guarantee sufficient full-cell balancing. Electrodes with a diameter of 11 mm (≡0.95 cm^2) were punched out and compressed to ≈30% porosity with a KBr press.

Graphite electrodes were prepared by mixing graphite (commercial, T311, SGL Carbon, Germany) and PVdF at a mass ratio of 95/5 with NMP by applying the same procedure as for the cathode electrodes. The graphite ink was coated onto copper foil (MTI, 12 μm) and dried in a convection oven at 50°C for 3 h. The loading of the graphite coating was ≈6 $mg_{graphite}$/cm^2, corresponding to ≈2.05 mAh/cm^2 (based on a specific capacity of ≈340 mAh/g). The electrodes were punched out with a diameter of 11 mm and compressed to a porosity of ≈30%.

Prior to cell assembly (OEMS & Impedance), anodes were dried under dynamic vacuum at 120°C. The cathodes were dried at 25°C (for the freeze-dried material), at 80°C (for the CAM which was dried at 80°C prior to coating), or at 120°C for all other samples for at least 12 h in a vacuum oven (Büchi, Switzerland) under dynamic vacuum, and then transferred into an argon-filled glove box (MBraun, Germany) without exposure to air.

On-line electrochemical mass spectrometry (OEMS).—For OEMS experiments, cathode electrodes were coated onto a stainless-steel mesh (see above), as this porous current collector allows for fast diffusion of evolved gases from the electrode to the flow-restricting capillary leak into the mass spectrometer.[38] The design of the here used custom-made one-compartment OEMS cell as well as the OEMS setup were reported previously.[39] OEMS cells were assembled with a 17 mm diameter lithium metal (from Rockwood Lithium, USA) counter electrode, one glassfiber separator (200 μm thickness, VWR, Germany), an NCM working electrode, and 120 μl of electrolyte composed of EC-only with 1.5M $LiPF_6$ (BASF SE, Germany). The cells were connected to the mass spectrometer, held for 4 h at OCV (open circuit voltage), and then charged to 5.0 V vs. Li^+/Li at a C/10 rate (C-rates here are referenced to a nominal capacity of 275 mAh/g for complete delithiation). For quantification of the mass spectrometer currents, a calibration gas containing O_2 and CO_2 (each 2000 ppm) in Argon (Linde AG, Germany) was used. All currents were normalized to the current at m/z = 36 (Ar isotope) in order to correct for effects of minor pressure and temperature changes. The currents m/z = 32 (O_2) and m/z = 44 (CO_2) were converted into gas concentration using the cell volume (≈10 mL) and the ideal gas law.

On-line mass spectrometry (OMS).—The above described OEMS setup was modified such that the gas evolution upon the addition of deionized water to the pristine NCM-851005 powder could be examined. For this, the OEMS cell was replaced by a Swagelok T-fitting: one end was connected to the flow-restricting capillary of the MS system, one was equipped with a septum in order to be able to introduce water with a syringe, and one was sealed with a standard closed nut into which 0.5 g NCM-851005 powder had been added (see inset of Figure 6). The cell was assembled in the glove box and then connected to the flow-restricting capillary of the MS system. Following a 40 minutes rest phase, argon was injected with a syringe in order to check for the tightness of the septum during the injection process. After 60 minutes of recording the mass traces of O_2, H_2O, and N_2, 2.5 mL of purified water were injected into the cell onto the NCM powder while continuing to monitor the mass signals.

Electrochemical impedance spectroscopy (EIS) and charge/discharge cycling.—The impedance of the cathode was measured with a micro-reference electrode based on our previously introduced gold wire reference electrode (GWRE) which is integrated into a standard Swagelok T-cell.[40] After assembly of the cell with a graphite counter electrode, an NCM-851005 working electrode, the GWRE, two glass fiber separator, and 60 µl of LP57 electrolyte (from BASF SE, Germany), the GWRE was lithiated using the NCM-851005 working electrode (1 h at 150 nA, consuming only ≈0.005% of its capacity). Before measuring the cathode impedance, two formation cycles of the graphite/NCM-851005 full-cells were carried out at 25°C between 4.2–3.0 V cell voltage at a rate of C/10 (referenced to 215 mA/g for the first charge). The formation protocol consisted of a constant-current constant-voltage (CCCV) charge with a cutoff for the CV phase at C/20 and a constant-current (CC) discharge. After formation, the cells were charged to 50% SOC by a 5h charge with C/10 based on the second-cycle discharge capacity. After 1h of an OCV rest phase, the cathode impedance was recorded in potentiostatic mode from 100 kHz to 100 mHz with a voltage perturbation of 10 mV. Afterwards, charge/discharge cycling at 25°C for another 198 cycles was carried out with a CCCV charge to 4.2 V with C/2 (cutoff for the CV phase at C/20) and a CC discharge to 3.0 V with 1C.

X-ray photoelectron spectroscopy (XPS).—Surface analysis of the pristine and twice washed NCM-851005 (dried at 180°C) was carried out by X-ray photoelectron spectroscopy (Axis, Supra, Kratos, UK). The powders were pressed to pellets inside an argon-filled glove box and mounted onto an electrically insulated sample holder, which can be transferred from the glove box into the XPS system without any air exposure using a transfer chamber (Kratos, UK). The sample was kept in the ante-chamber of the XPS until a pressure of $\approx 10^{-8}$ Torr, and was then transferred to the sample analysis chamber (SAC), where the pressure was always kept below $\approx 10^{-9}$ Torr during the whole measurement period. Sample irradiation was carried out with a monochromated Al K_α radiation (1486.6 eV) with an emission current of 15 mA. Survey spectra were recorded for all samples with a stepsize of 0.5 eV and a pass energy (PE) of 160 eV. Detailed spectra were recorded with a stepsize of 0.2 eV and a pass energy of 20 eV. For all measurements, a charge neutralizer was used, and the spectra were calibrated to the adventitious carbon peak with a binding energy (BE) of 284.8 eV.

Thermogravimetric analysis with coupled mass spectrometry (TGA-MS).—For TGA-MS analysis, a TGA system (Mettler Toledo, Switzerland) coupled to a mass spectrometer (Pfeiffer Vacuum, Germany) was used. All samples analyzed by TGA-MS were dried in a vacuum oven (Büchi, Switzerland) for at least 3 h at 120°C under dynamic vacuum. Both pristine NCM-851005 and twice washed NCM-851005 (washed in ambient air) dried at 120°C after washing were analyzed with the following protocol: First, the TGA-MS was flushed at 25°C for 10 minutes with an argon flow rate of 200 mL/min, followed by reducing the argon flow rate to 20 mL/min for 10 minutes. After these pre-treatment steps the TGA-MS analysis was initiated, ramping the temperature from 25°C to 120°C at 10 K/min, where it was held for 40 minutes. The actual measurement step was a subsequent temperature ramp at 10 K/min to 450°C, followed by a temperature hold phase of 50 minutes. The O_2 (m/z = 32) mass traces from the MS were normalized to the nitrogen signal (m/z = 28). The H_2O (m/z = 18) mass traces were normalized to the first measurement point (no normalization on the nitrogen signal).

Results

Li_2CO_3 & LiOH release and pH-value during washing of NCM-851005.—To study the washing process, we selected the Ni-rich cathode material NCM-851005, as it is known that the formation of surface contaminants, such as LiOH and Li_2CO_3, is most pronounced and has the most detrimental effect on cycle-life for nickel-rich materials.[8,9,22] In order to obtain accurate values for the amounts of adsorbed LiOH and Li_2CO_3 from the titration analysis of the filtrate after the first washing step as well as for their possible formation in the second washing step, the washing process for the following set of washing experiments was carried out in an argon-filled glove box in order to exclude any effects of CO_2 from the air.

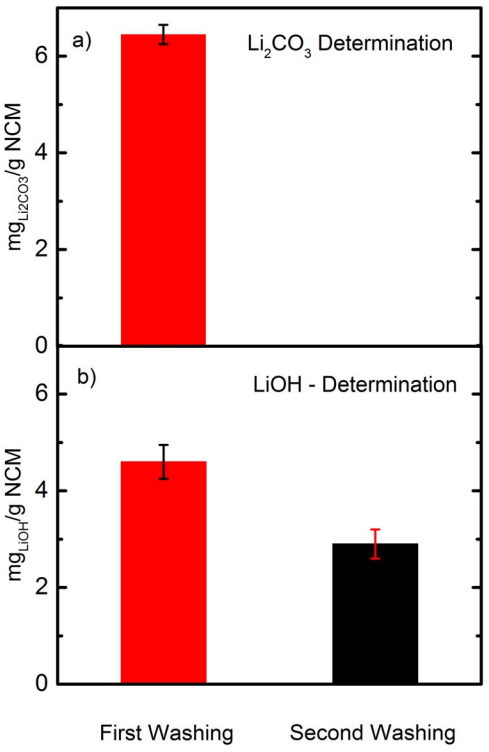

Figure 1. Amounts of a) Li_2CO_3 and b) LiOH determined in the filtrate after the first (red bars) and the second (black bar) washing of NCM-851005 with deionized and degassed water. For each washing step, conducted under argon atmosphere at room temperature, 20 g NCM-851005 powder was mixed with 100 mL deionized and degassed water for 20 minutes, and the carbonate and hydroxide amounts were determined by titration with HCl. The error bars show the standard deviation of three repeat measurements.

Figure 1a shows the lithium carbonate content determined by titration of the washing filtrate. After the first washing step, the amount of lithium carbonate in the wash solution is found to be 6.4 ± 0.2 mg_{Li2CO3} per gram NCM (red bar). This would correspond to ≈0.64 wt% Li_2CO_3 on the surface of the NCM-851005 material (assuming Li_2CO_3 to be the main carbonate species), roughly 2-fold lower than the carbonate impurities of ≈1.5 wt% reported by Noh et al.[22] for their 85% nickel containing NCM material ($LiNi_{0.85}Co_{0.075}Mn_{0.075}O_2$), quantified by an analogous titration method. The differences in Li_2CO_3 content can be due to differences in the synthesis process, the storage conditions of the as-synthesized CAM, and the specific surface areas of the materials. Following the first washing step and drying of the NCM-851005 material in a vacuum oven in the glove box, a second washing step was conducted. Interestingly, no more Li_2CO_3 can be detected in the wash solution after the second washing step, which suggests that owing to the high solubility of Li_2CO_3 in water, the long washing time and the high water/CAM ratio were sufficient to quantitatively remove all Li_2CO_3 impurities within the first washing step under argon atmosphere.

The LiOH content determined by titration after the first washing step is shown in Figure 1b, corresponding to 4.6 ± 0.35 mg_{LiOH} per gram NCM (red bar) or ≈0.46 wt% (assuming LiOH to be the main hydroxide species); in terms of molar quantities, this corresponds to 0.019 ± 0.001 $mol_{LiOH}/mol_{NCM\text{-}851005}$ based the molecular weight of 97.4 $g/mol_{NCM\text{-}851005}$. This again is roughly 2-fold lower than the ≈1.1 wt% reported by Noh et al.[22] for their $LiNi_{0.85}Co_{0.075}Mn_{0.075}O_2$ material. Generally, one would expect that

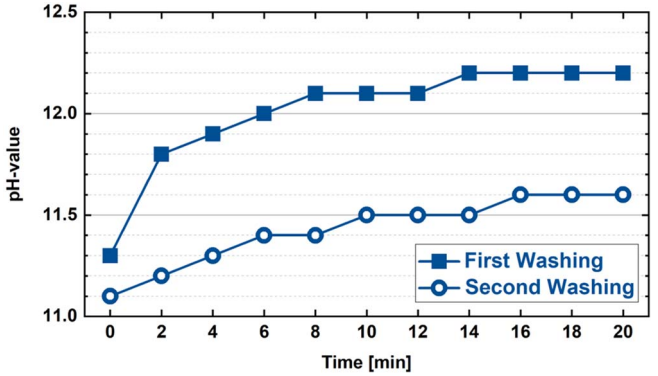

Figure 2. Progression of the pH-value over time for a suspension of 20 g NCM-851005 in 100 mL deionized and degassed water while stirring in an argon-filled glove box. The solid squares show the pH-value when pristine NCM-851005 powder is being washed for the first time; the open circles show the pH-value during the second washing of the NCM-851005 powder.

after the first washing step all of the LiOH surface impurities should be removed, as its solubility in water at room temperature is roughly 10-fold higher than that of Li_2CO_3. Surprisingly, however, the LiOH content in the filtrate of the second washing step was still very high, namely 2.8 ± 0.15 mg_{LiOH} or ≈0.28 wt% (black bar), equating to 0.011 ± 0.001 $mol_{LiOH}/mol_{NCM\text{-}851005}$. As LiOH surface impurities must have been removed in the first washing step, this additional amount of LiOH must be produced by the washing process itself, presumably by H^+/Li^+ ion exchange between the solution and the NCM-851005, as will be discussed later. In this case, the total molar fraction of Li^+ lost from the bulk/near-surface of the NCM-851005 material over the two washing steps would range between ≈1.1 mol%, if the LiOH in the first washing step would be exclusively from LiOH surface contaminants, and ≈3.0 mol% (i.e., sum from first and second washing step), if no LiOH surface impurities had been present on the pristine NCM-851005 material. This means that during the two washing steps up to ≈3 mol% of lithium could be lost from the bulk/near-surface of the NCM-851005 material.

The dissolution and to a certain extent formation of LiOH are also reflected in the change of the pH-value of the wash solution during the first and second washing under argon, as is shown in Figure 2. Upon addition of pristine NCM-851005 powder to the wash solution for the first time (solid squares), the pH immediately jumps to a value of ≈11.3, and over the course of 20 minutes approaches an essentially constant value of ≈12.2. When the once washed and then dried NCM-851005 powder is subjected to a second washing step, the pH immediately jumps to a value of ≈11.1 (open circles), similar as in the first washing step, but then levels off at a lower value of ≈11.6 after 20 minutes. While the rapid initial pH increase in the first washing process could be ascribed to the dissolution of LiOH surface contaminants, this is unlikely the case for the second washing process, due to the high water solubility of LiOH. Analogous pH vs. time traces and an analogous lower wash solution pH for a washed Ni-rich CAM were already observed by Kim et al.[24] for NCA with 83% Ni and by Xiong et al.[26] for NCM811. This implies that an initially fast chemical reaction must happen, which over the course of time becomes limited by a slower diffusion process (note that ion transport in the aqueous phase is not expected to be limiting, as the solution was stirred).

The above observed release of Li_2CO_3 and LiOH during the first washing step (Figure 1) accompanied by a rapid pH increase (Figure 2) is consistent with a dissolution and removal of Li_2CO_3 and LiOH surface impurities from the surface of the NCM-851005 material. However, the continuous more gradual increase of the pH after its initial rapid increase in the first washing step as well as the release of LiOH in the second washing step, despite its higher solubility compared to Li_2CO_3 that can only be found in the first washing step does suggest a slow but gradual ion exchange between lithium ions from the bulk/near-surface of the NCM structure with protons from the water phase, producing LiOH dissolved in the aqueous phase, resulting in the observed rise in pH:

$$Li^+|_{NCM} + H_2O \rightarrow H^+|_{NCM} + Li^+ + OH^- \quad [1]$$

In recent work, Shkrob et al.[7] showed by synchrotron XRD and other analytical methods that an Li^+/H^+ exchange indeed occurs upon the long-term exposure of NCM-523 to moist air with 100% relative humidity. While their data are not consistent with the formation of a pure γ-NiOOH phase that Moshtev et al.[41] had proposed to be a possible reaction product of $LiNiO_2$ and H_2O, the analysis by Shkrob et al.[7] suggests a substantial partial ion exchange constituting a sort of intermediate of the pure hydrous oxide phase. Very recently, Jeong et al.[42] published a study on the effect of washing/drying on the surface properties and the cycle-life of $LiCoO_2$ (LCO) cathode active materials, providing very strong evidence for the near-surface formation of CoOOH, as a result of an Li^+/H^+ ion exchange. In summary, the above discussion suggests that significant Li^+/H^+ ion exchange is occurring when Ni-rich NCMs or NCAs as well as LCO are mixed with water, producing a near-surface layer with varying Li^+/H^+ ratios in the layered oxide structure.

Effect of washing/drying on the first-cycle gas evolution and the cathode impedance.—To examine the effect of washing/drying on the surface properties and the electrochemical performance of NCM-851005, the NCM-851005 material washed twice under argon was heated under vacuum to 180°C in order to remove residual water. Whether this would remove residual reactive lithium from the NCM particle surface was then analyzed via XPS, while the effect of washing/drying on the gas evolution in the first charge cycle was determined by on-line electrochemical mass spectrometry (OEMS). Finally, the effect of washing/drying on the cathode charge-transfer resistance was evaluated by electrochemical impedance spectroscopy (EIS) using a gold wire reference electrode (GWRE).

In order to prove that no more residual lithium salts (i.e., LiOH and Li_2CO_3) remain on the NCM surface after washing, as claimed by Kim et al.,[24] we performed XPS measurements of the pristine NCM-851005 material and the NCM-851005 that was washed twice under argon and was then vacuum dried at 180°C. The samples were transferred to the vacuum system of the XPS without any exposure to air, using a transfer chamber (Kratos). The Li 1s region was recorded from 52–58 eV binding energy (BE). The top panel of Figure 3 shows the spectrum of the as-received pristine NCM-851005 material. It clearly exhibits two peaks, one centered around 54.0 eV (in green) that we attribute to the intercalated lithium ($Li_{intercalated}$), and one centered around at 55.3 eV (in blue) that we attribute to lithium salts (i.e., Li_2CO_3 and LiOH) on the surface of the pristine NCM-851005 particles ($Li_{surface}$). The assignment of the peaks was further validated by storing the as-received material in humid air, which resulted in a strong increase of the surface lithium peak (data not shown). On the other hand, when the NCM-851005 powder is washed twice under argon, no more surface lithium can be detected by XPS, whereas the intercalated lithium peak (in green) is still present (see lower panel of Figure 3). This result fits well with the report by Kim et al.,[24] who showed by means of FTIR (Fourier transform infrared) spectroscopic measurements that the amounts of LiOH and Li_2CO_3 drastically decrease after washing of NCA with 83% Ni. Thus, washing clearly leads to a decrease in residual LiOH and Li_2CO_3 on the surface of Ni-rich CAMs.

Next, we will evaluate whether the washing/drying process has any influence on the initial gassing and the impedance of the NCM-851005 material. Recently, it has been shown that oxygen released from the lattice of nickel-rich layered materials at high degree of delithiation (i.e, at high SOC) reacts with the electrolyte, leading to strong gas evolution during the first cycles and to pronounced capacity fading over extended charge/discharge cycling.[20,27,29] Furthermore, it has been shown that hydroxide species on NCM surfaces react with the electrolyte, accompanied by the formation of CO_2 during storage of fully lithiated NCMs in the electrolyte at elevated temperature.[8,20] In order to investigate the effect of washing/drying on the gas

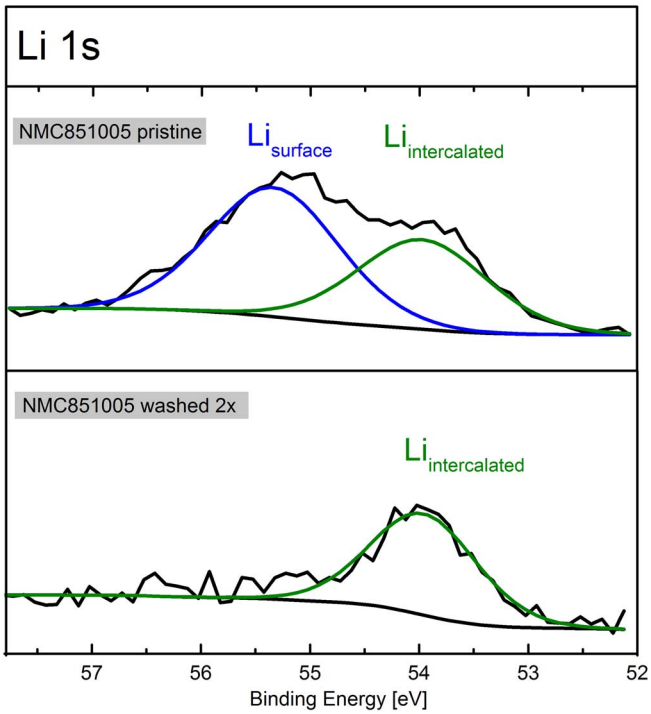

Figure 3. XPS data (in black) from the Li 1s region of as-received pristine NCM-851005 dried under vacuum at 120°C (upper panel) and of NCM-851005 washed twice under argon and then dried under vacuum at 180°C (lower panel). The samples were transferred from the glove box to the XPS chamber without any air exposure using a transfer chamber. For peak fitting, a Shirley background (black dashed line) was subtracted and two peaks (fitted with a Gauss-Lorentz function (blend = 0.3)) with a peak binding energy of 54.0 eV ($Li_{intercalated}$; green line) and 55.3 eV ($Li_{surface}$; blue line) and with a FWHM of 1.4 were used.

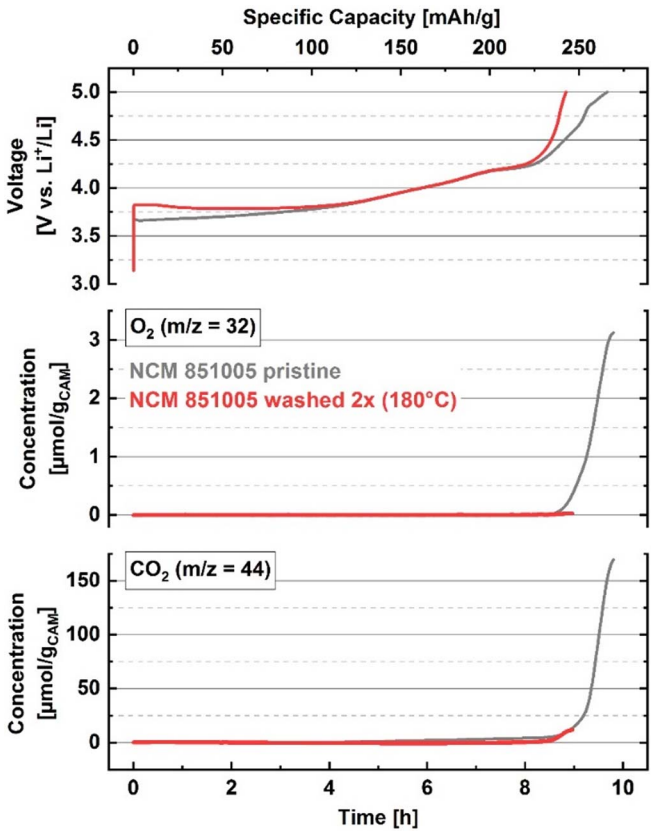

Figure 4. OEMS measurements of the first lithiation cycle to 5.0 V using Li/NCM-851005 half-cells with the pristine (red lines) and the twice washed NCM-851005 (washed under argon and dried at 180°C; gray lines). Upper panel: charge voltage vs. time and capacity at a C/rate of C/10 (referenced to 275 mAh/g theoretical delithiation capacity). Middle/lower panels: evolution of the concentrations of evolved O_2/CO_2 given in units of $\mu mol/g_{CAM}$. Cells were charged at 25°C, using a metallic Li counter electrode, a glassfiber separator, and an EC-only electrolyte with 1.5M $LiPF_6$.

evolution of a nickel-rich NCM material in the first charge to high SOC, we performed on-line electrochemical mass spectrometry (OEMS) on electrodes with the pristine and the washed NCM-851005. For this, we used a model electrolyte based on pure EC mixed with 1.5 M $LiPF_6$, as it offers two experimental advantages: i) due to its low vapor pressure, an increased signal to noise ratio in the OEMS experiments can be obtained;[43] ii) the only gases that evolve during EC reduction on the lithium counter electrode are CO and ethylene,[44–46] which can be clearly differentiated from the O_2 and CO_2 evolved from the cathode material.[29]

Results of the OEMS measurements on both samples are shown in Figure 4. The upper panel shows the galvanostatic charge profiles from OCV (≈3 V) up to 5.0 V versus a Li counter electrode, and the middle/lower panels depict the concentration of the concomitantly evolved O_2 (m/z = 32, middle panel) and CO_2 (m/z = 44, lower panel) in units of $\mu mol/g_{CAM}$. The galvanostatic charge profile and the gas evolution for the pristine NCM-851005 is depicted by the gray lines in Figure 4, showing a capacity of ≈267 mAh/g during the first charge to 5.0 V vs. Li^+/Li. The onset for O_2 evolution can be observed at ≈84% SOC (corresponding to ≈4.32 V vs. Li^+/Li), which is consistent with the results reported by Jung et al.[20,27] for NCM811 and by Teufl et al.[30] for HE-NCM. Concomitant with the onset for O_2 evolution, a sharp increase in the CO_2 evolution can be observed. In contrast to that, the electrode made from the washed NCM-851005 (red lines in Figure 4) shows nearly no gassing up to 5.0 V vs Li^+/Li, i.e., essentially no O_2 and very little CO_2 evolution.

The oxygen release for the pristine NCM-851005 in Figure 4 (middle panel) is in accordance with Streich et al.[28] and with our previous studies, in which we had shown that the release of lattice oxygen from layered oxides occurs at SOC's exceeding roughly 80%.[20,27,28,30,38,47] However, concerning the CO_2 evolution during the first charge of layered oxides, there is an ongoing debate about its origin: i) Luo et al.[48] assumed that the evolved CO_2 is entirely due to electrolyte oxidation with lattice oxygen; ii) Renfrew et al.[19] proposed the opposite, suggesting that CO_2 evolution is exclusively triggered by the oxidative decomposition of Li_2CO_3 from surface regions, a statement which was somewhat revised in their later work.[49] Furthermore, they recently showed that soaking NCM-622 in water can effectively lower the residuals (e.g. Li_2CO_3 and LiOH) on the surface and thus lower the gassing during cell formation;[50] iii) Jung et al.[27,29] suggested that the CO_2 evolved at ≈4.2 V vs. Li^+/Li is produced from surface impurities, while CO_2 evolved upon lattice oxygen release at higher potentials would be due to a reaction with the carbonate electrolyte. Recently, Jung et al.[20] conducted temperature dependent measurements with a ^{13}C labeled electrolyte and NCM622 to better understand the origin of the CO_2 evolution at different potentials, revealing a reaction of surface hydroxides with the electrolyte at low potentials as well as a strong reaction of lattice oxygen with the electrolyte and of the resulting acidic electrolyte decomposition species with Li_2CO_3 surface contaminants at >4.3 V vs. Li^+/Li.[20,51] For the following discussion, we will adopt the mechanistic view proposed by Jung et al.,[20] who show that the decomposition of Li_2CO_3 surface contaminants occurs at the onset of O_2 evolution. For this reason, the removal of Li_2CO_3 surface contaminants by washing (see Figure 1a) should lower the overall CO_2 gassing at high potentials, as already shown for Ni-rich NCAs with 83–85% Ni.[24,25] Here, however, one must mention that the electrodes with the washed NCM-851005 were coated at ambient atmosphere, so that small amounts of Li_2CO_3 might have been re-formed on its surface prior to cell assembly. As expected, and

as mentioned above, the difference in the amount of evolved gases between the washed and the pristine NCM-851005 is quite striking (see Figure 4). By the end of the first charge to 5.0 V vs. Li^+/Li, a total amount of ≈3.1 $\mu mol/g_{CAM}$ O_2 and ≈171 $\mu mol/g_{CAM}$ CO_2 are evolved from the pristine NCM-851005, in stark contrast to only ≈0.025 $\mu mol/g_{CAM}$ O_2 and ≈12 $\mu mol/g_{CAM}$ CO_2 that are evolved from the washed NCM-851005 (capacity ≈244 mAh/g), corresponding to a ≈14-fold lower total gas evolution for the washed/dried NCM-851005. While one could argue that the reduced amount of evolved CO_2 after washing of the NCM-851005 might solely be due to a removal of most of the Li_2CO_3 surface contaminants (if the ≈12 $\mu mol/g_{CAM}$ evolved CO_2 were entirely due to the decomposition of Li_2CO_3 surface contaminants, it would correspond to a reasonable value of ≈0.09 wt%), the roughly two orders of magnitude lower O_2 evolution of the washed NCM-851005 indicates that the surface of the washed NCM-851005 has undergone changes beyond a simple removal of hydroxide and carbonate surface impurities.

As was proven unambiguously by a combination of OEMS and transmission electron microscopy (TEM) in the case of HE-NCM, lattice oxygen release is accompanied by the formation of an oxygen-depleted surface layer, which can restructure into a spinel-like surface layer.[30] Based on OEMS studies, an analogous phenomenon was suggested for NCMs,[27,28] consistent with the observation of spinel/rocksalt surface layers by TEM measurements after cycling to high potentials and/or high SOC.[22,52] With this in mind, it is conceivable that the almost complete absence of oxygen evolution from the washed NCM-851005 dried at 180°C (see Figure 4) might be caused by the formation of an oxygen-depleted surface layer during the washing/drying process, stabilizing the NCM surface at high SOC. Incidentally, this type of mechanisms has recently been proposed by Jeong et al.[42] for washed/dried LCO. In this case, the generally expected increase of the impedance of the cathode active material caused by a spinel/rocksalt-like surface layer would have to be observed for the washed/dried NCM-851005 cathode.[22,42,53] This will be examined in the following cathode impedance analysis.

In order to determine whether the impedance of the NCM-851005 cathode active material is increased by the washing/drying process, graphite/NCM-851005 cells were assembled with a gold wire reference electrode (GWRE).[40] This micro-reference electrode allows for the recording of artefact-free individual impedance spectra of both the anode and the cathode in full-cells. In this study, cells were assembled with pristine as well as with washed NCM-851005 (washed two times under argon) that was dried at 180°C under vacuum. Following two formation cycles at C/10 and 25°C between 3.0–4.2 V, the cells were charged at C/10 to 50% SOC referenced to the second discharge capacity (corresponding to ≈3.7–3.8 V cell voltage), where the impedance was recorded (see experimental section for further details). The impedance spectra of the different NCM-851005 cathodes are shown in Figure 5. The partially visible high frequency semi-circle observed in both spectra is attributed to a contact resistance ($R_{Contact}$) between the cathode coating and the aluminum current collector; the low-frequency semi-circle represents the charge-transfer resistance of the NCM-851005 cathode active material ($R_{Cathode}$). More details on this can be found in the work by Landesfeind et al.[54] The pristine NCM-851005 shows a small cathode charge-transfer resistance of $R_{Cathode}$ ≈ 5 Ωcm^2 (determined by an R/Q fit). When the same material is washed twice in water and dried under vacuum at 180°C, $R_{Cathode}$ increases by a factor of ≈4 to ≈20 Ωcm^2. As discussed above, the increase of $R_{Cathode}$ does suggest the formation of an oxygen-depleted and more resistive surface layer during the washing and/or drying process. Therefore, in the following, we will examine whether oxygen or oxygen-containing species are released during the washing and/or during the drying step of a washed material.

Release of oxygen-containing species during the washing and drying process.—Both, the OEMS data (Figure 4) and the cathode impedance data (Figure 5) suggest that the washing and/or the drying process may lead to an oxygen-depleted surface layer on the NCM-851005 particles. Therefore, we will first examine whether oxygen

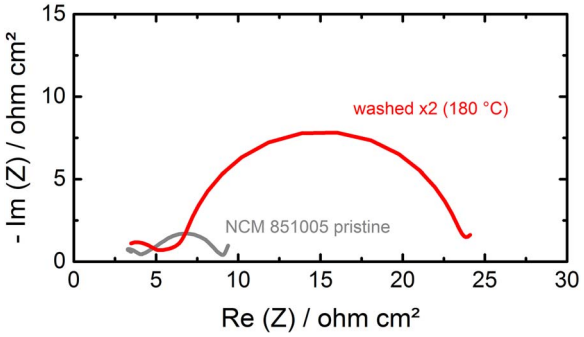

Figure 5. Impedance response of cathode electrodes with pristine NCM-851005 (gray) as well as with washed NCM-851005 (washed twice under argon) dried under vacuum at 180°C (red) at 50% SOC and 25°C. The cathode impedance spectra between 100 kHz and 0.1 Hz were measured in graphite/NCM-851005 full-cells using a gold-wire reference electrode (GWRE), and were recorded after two formation cycles with C/10 and a subsequent charge to 50% SOC (corresponding to ≈3.7–3.8 V cell voltage).

might be released during the washing process. Some evidence for this can be found in the literature. For example, Mosthev et al.[41] suggested that the extraction of Li^+ from $LiNiO_2$ cathode active material powder in an aqueous solution would be charge-compensated by the evolution of oxygen from the layered oxide lattice. Furthermore, Liu et al.[55] investigated the deterioration of $LiNiO_2$ powder under ambient air und suggested that Ni^{3+} from the lattice would be reduced to Ni^{2+}, with the corresponding oxidation reaction being the oxidation of the lattice oxygen to gaseous O_2. If either one of these processes were true, the addition of water to an NCM-851005 powder should lead to the evolution of O_2. In order to study this, we used a modified version of our current OEMS setup to conduct an on-line mass spectrometry (OMS) analysis during the washing process. For this, one part of a Swagelok T-fitting was connected to the capillary leading to the MS system (see inset in Figure 6). At one of the other connections, a septum was installed to allow the addition of controlled amounts of water with a syringe, while the remaining connection was equipped with a nut into which NCM-851005 powder was added.

After assembly of the cell in an argon-filled glove box, the mass traces of O_2 (m/z = 32) and of H_2O (m/z = 18) were recorded. The first 40 minutes consisted of a rest period where the signal of residual water decreases and the O_2 signal increases slightly. The increase of the oxygen signal is due to a small leakage of the cell (presumably through the septum), as by dividing the mass signal of N_2 (m/z = 28) by the oxygen signal, a constant time-independent response is obtained, which clearly indicates the slow intrusion of air. After the rest period of 40 minutes, ≈2.5 mL of pure argon (taken from the glove box atmosphere) is injected into the cell in order to verify the tightness of the septum after an injection. One can nicely see that during the penetration of the septum with the needle of the syringe, no increase in the oxygen or water masses are observed. After a total of 100 minutes, 2.5 mL of water are injected onto the 0.5 g of the pristine NCM-851005 powder, corresponding to the same water/CAM ratio as in our washing experiments. Consequently, the mass trace for water increases (blue line in Figure 6), but the O_2 mass trace (red line) does not increase, clearly indicating that no oxygen evolution occurs when water is added to NCM-851005. Therefore, there is no release of lattice oxygen in form of molecular oxygen from a nickel-rich NCM during washing with water, contrary to the above discussed assumptions in the literature.

Based on the suggested Li^+/H^+ exchange (see Equation 1), a NiOOH-like structure would be expected to be formed in the near-surface region of the Ni-rich NCM-851005 particles upon washing. For pure NiOOH, it is known from the literature that it is thermally unstable: at already ≈80°C it starts to lose water from the interlayers, and at ≈260°C it is being partially converted to NiO, accompanied by the release of water and oxygen, whereby full conversion to the

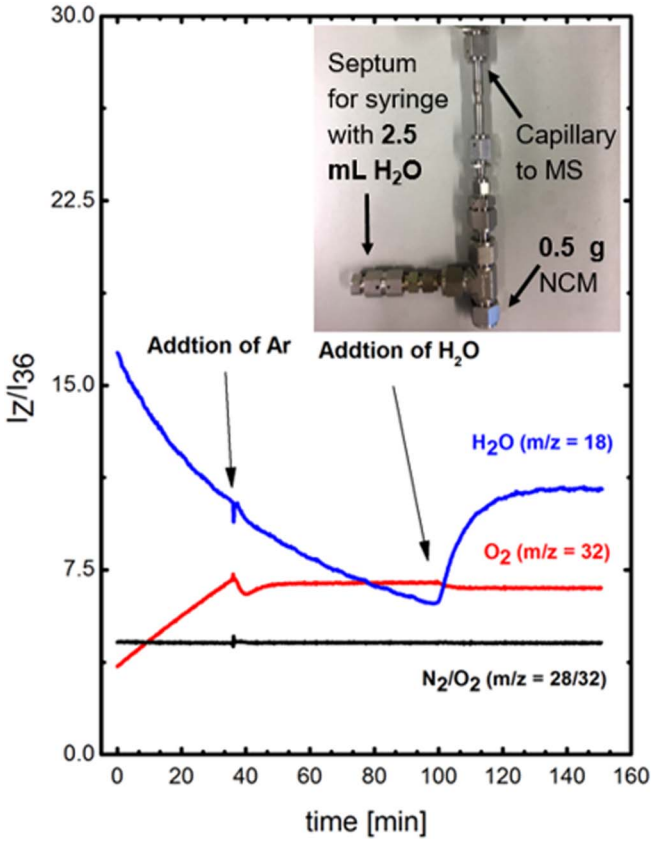

Figure 6. Mass traces of O_2 (m/z = 32, in red), H_2O (m/z = 18, in blue) and of the N_2/O_2 ratio (m/z = 28/32, in black) recorded using a modified Swagelok T-cell connected to the MS capillary inlet and containing 0.5 g pristine NCM-851005 powder, placed at the bottom part sealed with a nut (see inset). The first 40 minutes consisted of a rest phase, followed by the addition of pure argon with a syringe through the septum in order to check the stability of the septum. After further 60 minutes (at t = 100 min), 2.5 mL water were injected with a syringe onto the NCM-851005 powder, and the mass traces were recorded for further 60 minutes.

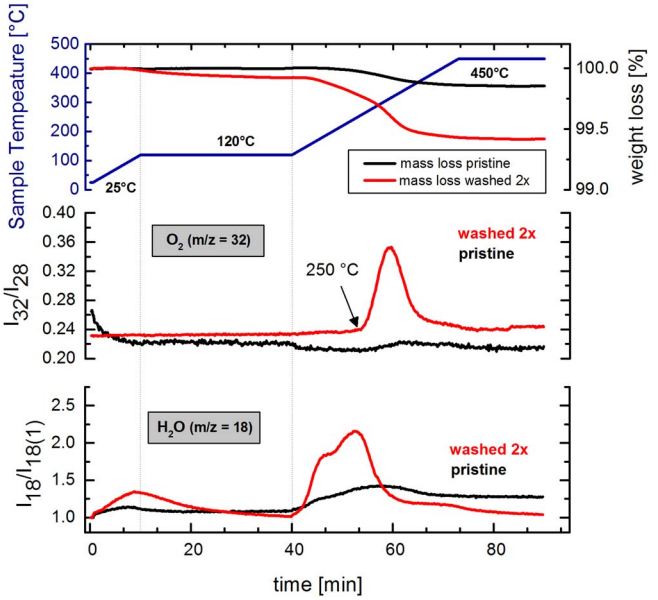

Figure 7. TGA-MS analysis under argon (20 mL/minute) of pristine NCM-851005 (black lines) and of washed NCM-851005 (twice under argon) that was dried at 65°C under vacuum after each washing step (red lines). All materials were dried prior to TGA-MS experiments at 120°C under dynamic vacuum for at least 3 h. Top panel: temperature vs. time program with heating ramps and hold phases (blue line, left y-axis) and corresponding mass losses of the pristine and washed NCM (right y-axis). Middle panel: O_2 signal (m/z = 32) normalized by the nitrogen signal (m/z = 28) in order to exclude artefacts from minute air leaks. Bottom panel: mass traces of water H_2O (m/z = 18) normalized by their respective values at the beginning of each measurement sequence (i.e., after the pre-treatment program).

rocksalt NiO structure is completed at ≈600°C.[56] The complete thermal reduction of the Ni^{+3} in the NiOOH phase to Ni^{+2} in the NiO rocksalt phase is given as:

$$2\,NiOOH \;\rightarrow\; 2\ \text{"NiO"} + 0.5\,O_2 + H_2O \qquad [2]$$

Based on the described thermally induced transformation of NiOOH, we would expect that heating an NCM-851005 material with a partially Li^+/H^+ ion exchanged near-surface region formed during washing would lose water and oxygen upon heating. This has actually already been reported for $LiCoO_2$ (LCO) by Jeong et al.,[42] who showed that washing of an LCO cathode active material with water leads to a CoOOH like structure, which is then thermally decomposed to either a thin CoO surface layer when dried under air at 400°C or to a thicker Co_3O_4 surface layer when air-dried at 700°C. For the latter treatment, the LCO cathode impedance was found to increase substantially.

To further investigate the drying process of washed NCM-851005, which was conducted under vacuum in our experiments (see experimental), we carried out a TGA-MS analysis under a pure argon stream of a pristine and a washed NCM-851005 (washed twice under argon) that was dried under vacuum at 120°C during/after washing. Prior to TGA-MS analysis, the NCM samples were dried at 120°C under dynamic vacuum for at least 3h. The TGA-MS protocol consisted of a pre-treatment at 25°C to remove physiosorbed water (10 minutes at an argon flow rate of 200 mL/min, followed by 10 minutes at an argon flow rate of 20 mL/min). The actual TGA-MS experiment shown in Figure 7 then was conducted at an argon flow rate of 20 mL/min: first, a temperature ramp to 120°C at 10 K/min, then a 40 minute hold phase at 120°C, and finally a temperature ramp to 450°C (10 K/min), holding the final temperature for another 20 minutes (see blue line in the upper panel of Figure 7). The results of this experiment are shown in Figure 7. Since the samples were dried at 120°C prior to the TGA-MS experiment, no mass losses and only minor amounts of water release were observed during the first temperature ramp from 25°C to 120°C (see Figure 7). When ramping the temperature from 120°C to 450°C, the pristine NCM-851005 shows a total mass loss of only ≈0.1 wt% that initiates at ≈200°C (top panel, black line), accompanied only by a weak MS signal for water (bottom panel) and a noticeable absence of O_2 release (middle panel). On the other hand, tor the washed NCM-851005, the onset of a first mass loss can be observed somewhat earlier, at ≈150°C (red lines in Figure 7), accompanied by the release of water and an albeit very weak MS signal for released O_2. In stark contrast to the pristine NCM-851005, the washed material shows a pronounced release of O_2 that initiates at ≈250°C, with a maximum release rate at ≈310°C (middle panel). This suggests a two-step thermal decomposition reaction for the washed NCM-851005, namely one initiating at ≈150°C caused by the release of predominantly H_2O, and one initiating at ≈250°C upon the release of predominantly O_2. This seems to be similar to the above described stepwise release of first H_2O at ≈80°C and of H_2O together with O_2 at ≈260°C for NiOOH, as reported by Pan et al.;[56] it is also reminiscent of findings by Bak et al.,[57] who reported the initial formation of a disordered M_3O_4-type spinel upon heating of partially delithiated NCM-811 ($Li_{0.22}Ni_{0.8}Co_{0.1}Mn_{0.1}O_2$) to ≈150°C,[57] which upon further heating was shown to decompose to an MO rocksalt phase that is fully formed at ≈360°C. In analogy, it is reasonable to assume that the thermal decomposition of an H^+-exchanged Ni-rich NCM (i.e., an essentially delithiated NCM in the near-surface region) may also be described in terms of these two principal processes: i) the initial formation of a disordered M_3O_4-tupe

spinel at ≈80–150°C according to

$$MOOH \rightarrow \frac{1}{3} M_3O_4 + \frac{1}{2} H_2O + \frac{1}{12} O_2 \quad [3]$$

where mostly H_2O is being released; ii) the subsequent release of O_2 at ≈250–360°C, resulting in an MO-type rocksalt structure according to

$$M_3O_4 \rightarrow 3\,MO + \frac{1}{2} O_2 \quad [4]$$

The above hypothesized two-step process during drying would be consistent with the two different transition regions vs. temperature observed for the washed NCM-851005 in Figure 7 (i.e., one starting at ≈150°C and one at ≈250°C). Furthermore, the formation of an oxygen-depleted spinel-type surface layer on the washed NCM-851005 dried at temperatures near ≈150°C would also be consistent with the reduced gassing of O_2 and CO_2 at high SOC levels observed by OEMS for the washed NCM-851005 dried at 180°C (Figure 4, red lines) and with its increased impedance (see Figure 5).

Effect of the drying temperature after washing on electrochemical characteristics.—If the above proposed reaction sequence were true, increasing the drying temperature of washed NCM-851005 would be expected to lead to a reduced gas evolution (O_2 and CO_2) during the first delithiation cycle and to higher cathode active material impedances, since the initially formed MOOH-like phase would gradually be decomposed at higher temperatures to less conductive M_3O_4 and ultimately to highly resistive MO surface layers. In order to prove this, we have carried out further OEMS and impedance measurements with washed NCM-851005 (washed twice at ambient atmosphere) dried at different temperatures: one sample was freeze-dried and has seen a maximum final drying temperature of 25°C (12 h under dynamic vacuum), while other samples were dried at 80°C and at 300°C (again 12 h under dynamic vacuum).

The OEMS results for the first lithiation cycle are shown in Figure 8, together with those for the pristine NCM-851005 and the twice washed NCM-851005 (under argon) dried at 180°C (both already shown in Figure 4). Compared to the substantial release of O_2 (≈3.1 μmol/g) and CO_2 (≈171 μmol/g) by the pristine NCM-851005 over the first lithiation cycle, Figure 8 shows a much reduced O_2 (≈0.35 μmol/g) and CO_2 (≈90 μmol/g) evolution for the washed and freeze-dried sample that experienced a maximum final drying temperature of 25°C. At the higher drying temperature of 80°C, a further substantial decrease of the amounts of O_2 (≈0.1 μmol/g) and CO_2 (≈26 μmol/g) can be observed, pointing toward the initial thermal decomposition of the MOOH-like surface phase formed during washing, most likely analogous to the reported partial loss of water from NiOOH interlayers at ≈80°C. A corresponding water desorption signal can be observed in the TGA-MS experiment shown in Figure 7 (bottom panel, red line). This trend of lowered gas evolution during the first delithiation cycle continues for drying the twice washed NCM-851005 at 180°C (for O_2 ≈0.025 μmol/g and for CO_2 ≈12 μmol/g) and at 300°C, where OEMS cannot detect any O_2 evolution and reveals only very small amounts of evolved CO_2 (≈6 μmol/g). Based on the above proposed reaction sequence and the phases observed by Bak et al.[57] for the thermal decomposition of delithiated NCM-811 ($Li_{0.22}Ni_{0.8}Co_{0.1}Mn_{0.1}O_2$), one would expect that a drying temperature of 180°C should be sufficiently high to produce an M_3O_4 spinel-type phase (acc. to Eq. 3), while a drying temperature of 300°C should result in an MO rocksalt-type structure (acc. to Eq. 4).

In addition to the decreasing O_2 and CO_2 evolution in the first lithiation cycle with increasing drying temperature for washed NCM-851005, Figure 8 also shows that the first-cycle delithiation capacity decreases with increasing drying temperature: while the washed and freeze-dried sample have essentially the same delithiation capacity as the pristine NCM-851005 (≈266–270 mAh/g, i.e., close to the theoretical capacity of ≈275 mAh/g), the washed samples dried at 80-300°C have clearly lower delithiation capacities (≈237–246 mAh/g). For the freeze-dried sample, this suggests that the NCM particle surface still

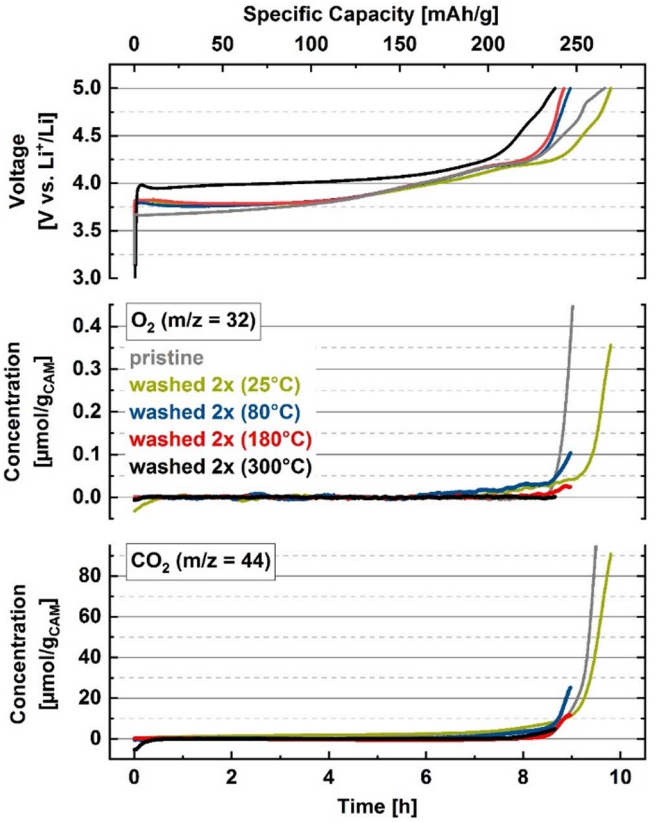

Figure 8. OEMS measurements of the first lithiation cycle to 5.0 V using Li/NCM-851005 half-cells with pristine and with twice washed NCM-851005 dried at different temperatures (for 12 h under dynamic vacuum; the material dried at 25°C was first freeze-dried). Upper panel: charge voltage vs. time and capacity at a C/rate of C/10 (referenced to 275 mAh/g theoretical delithiation capacity). Middle/lower panels: evolution of the concentrations of concomitantly evolved O_2/CO_2 given in units of $\mu mol/g_{CAM}$. Cells were charged at 25°C, using a metallic Li counter electrode, a glassfiber separator, and an EC-only electrolyte with 1.5M $LiPF_6$. Washing was conducted at ambient atmosphere, except for the sample dried at 180°C (for that, the data are the same as in Figure 4).

has a layered structure, without having trapped Li^+ in an inactive surface layer. On the other hand, the observed capacity loss of the washed NCM-851005 dried at ≥80°C, amounting to ≈20–30 mAh/g, is much larger than the estimated ≤3% Li^+ loss from the NCM particles during washing (based on the analysis of Figure 1), which would correspond to not more than ≈8 mAh/g. Therefore, we suggest that the lower capacity stems from a phase transformation into a lithium containing spinel and/or rocksalt surface phase, resulting in a loss of cyclable material; as will be shown later, this will also be reflected in the extended charge/discharge capacities of washed/dried NCM-851005. Similar surface phase transformations have been reported by Teufl et al.,[30] who observed a large capacity contribution from a spinel phase to the capacity of a Li- and Mn-rich NCM by a dQ/dV analysis; however, while for the Li- and Mn-rich NCMs the formed surface spinel phase can be charged/discharged reversibly at potentials of ≈3 V vs. Li^+/Li,[58,59] there is no evidence of such an electrochemically active spinel-type surface phase for the here examined Ni-rich NCM. Rather, we expect that lithium can get trapped within the surface phase, leading to a loss of lithium intercalation sites by the formation of an electrochemically inactive $(Li+M)_3O_4$ spinel-type surface phase or a (Li+M)O rocksalt-type surface phase.[57] As the formation of different surface phases should affect the charge-transfer resistance, we will next examine the impedance buildup of washed/dried NCMs.

The impedance of NCM-851005 cathodes using either the pristine or washed/dried NCM-851005 samples examined in Figure 8 was

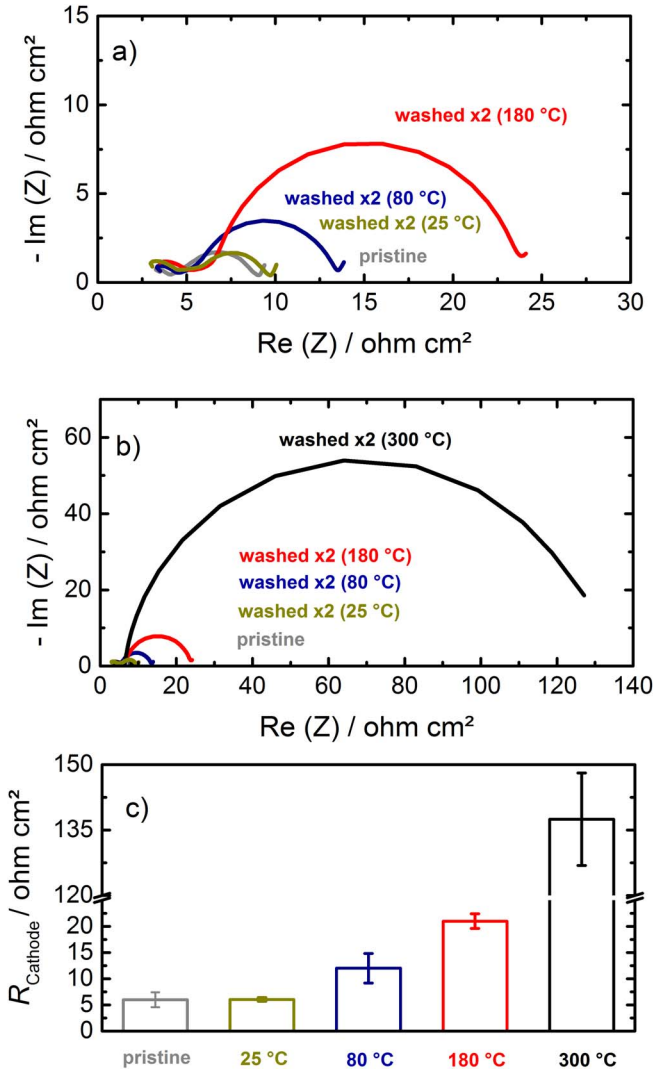

Figure 9. Cathode impedance spectra of the pristine and washed/dried NCM-851005 samples shown in Figure 8, measured with a micro-reference electrode (referred to as GWRE) in a graphite//NCM-851005 full-cell configuration at 50% SOC after two formation cycles at 0.1C and 25°C. a) Nyquist plot of the pristine NCM-851005 cathode (not washed, dried at 120°C, in gray), of the freeze-dried cathode (dried at 25°C, in green), of the cathode dried at 80°C (in blue), and of the cathode dried at 180°C (in red). b) Zoomed-out view of panel a) in order to accommodate the impedance data for a cathode dried at 300°C. The impedance was recorded from 100 kHz to 100 mHz with a perturbation of 15 mV at 25°C. c) Average NCM-851005 impedance (determined with a simple R/Q fit) from two independent measurements (i.e., from two cells) for each of the samples; the error bars indicate the minimum/maximum of two measurements.

determined in graphite/NCM-851005 full-cells by means of a micro-reference electrode (referred to as GWRE). The NCM-851005 cathode impedances ($R_{Cathode}$) at 50% SOC after two formation cycles are shown in Figure 9. The Nyquist plot features for all NCM-851005 samples shown in Figures 9a/9b are analogous to those already discussed in the context of Figure 5. Quite clearly, the resistance of the twice washed freeze-dried NCM-851005 sample that experienced a maximum drying temperature of 25°C ($R_{Cathode}$ ≈6 Ωcm^2, green bar in Figure 9c) is nearly unchanged from that of the pristine NCM-851005 ($R_{Cathode}$ ≈5 Ωcm^2, gray bar). This is consistent with the expectation that the MOOH-like surface layer produced by the near-surface Li^+/H^+ ion exchange of Ni-rich NCMs (see Eq. 1) will remain intact upon the removal of physisorbed water at/below room temperature, as is observed for pure NiOOH.[56] As the first lithiation cycle capacity of the pristine and the freeze-dried NCM-851005 are essentially identical (see Figure 8, upper panel), the intercalated protons must be deintercalated upon the first charge and then either react to HF with the $LiPF_6$ salt[60] or get reduced on the graphite anode to H_2 gas.[44] When increasing the drying temperature for the washed NCM-851005 to 80°C, the temperature at which pure NiOOH would lose interlayer water[56] and at which water desorption is also observed for the washed NCM-851005 (see Figure 7, red line in the lower panel), one can now observe an increase of the NCM-851005 impedance to a ≈2-fold higher value ($R_{Cathode}$ ≈10 Ωcm^2, blue bar in Figure 9c) compared to pristine NCM-851005. When the material is dried at 180°C, the cathode resistance increases by another factor of two to $R_{Cathode}$ ≈20 Ωcm^2 (red bar), which can be explained by the expected formation of an M_3O_4 spinel-like surface layer according to Eq. 3. Interestingly, when the washed NCM-851005 is dried at 300°C, i.e., above the temperature for which we had observed a substantial loss of oxygen in the TGA-MS experiment (Figure 7), its impedance drastically increases to $R_{Cathode}$ ≈130 Ωcm^2 (black bar).

Quite clearly, the above discussed impedance increase of washed NCM-851005 with drying temperature is amazingly consistent with the temperature-dependent phase transformations of delithiated NCM-811 ($Li_{0.22}Ni_{0.8}Co_{0.1}Mn_{0.1}O_2$) reported by Bak et al.,[57] who showed the formation of a disordered M_3O_4-type spinel at ≈135–150°C, which upon further heating would convert to an MO rocksalt phase that was fully formed at ≈360°C. This is reflected by the evolution of the impedance of washed NCM-851005 dried at different temperatures (Figure 9c): i) essentially unchanged impedance compared to pristine NCM-851005 when dried at low temperatures (here 25°C); ii) a significant impedance increase with drying temperatures between approximately 80–180°C, due to surface-spinel formation; and, iii) a dramatic impedance increase for drying at 300°C, due to the formation of a highly resistive rocksalt structure on the surface. Thus, these cathode impedance measurements underline that the drying temperature for washed Ni-rich NCMs is the main driver for reducing their gassing in a graphite/NCM full-cell, but also for increasing their impedance.

Influence of washing/drying on the full-cell cycling performance at 25°C.—Following the above described impedance measurements (Figure 9) conducted after formation (2 cycles at C/10 and a subsequent charge to 50% SOC), the graphite/NCM-851005 full-cells were cycled for another 198 cycles with a charge rate of C/2 to 4.2 V (CCCV mode, with a CV phase to C/20) and a discharge rate of 1C to 3.0 V (CC mode). The results of this test are shown in Figure 10, revealing that the discharge capacities and the capacity retention of the pristine NCM-851005 are superior to that of the washed NCM-851005, and that both capacities and capacity retention are the worse the higher the drying temperature.

Even during the first two formation cycles at C/10 with a 4.2 V upper cut-off potential (cycles 1 and 2 in Figure 10), the discharge capacities of the washed NCM-851005 cathodes are lower than those of the pristine material, particularly for the washed material dried at 300°C (see 2nd and 3rd columns of Table I). This reflects the lower first-charge capacities of the washed NCM-851005 cathodes already noted for the half-cell experiments shown in Figure 8, presumably due to the loss of lithium intercalation sites by the formation of an electrochemically inactive surface layer. We believe that the latter is responsible for the increasing cathode impedance of the washed NCM-851005 with increasing drying temperature (see Figure 9c), which manifests itself by an increasing discharge capacity loss when increasing the discharge rate from C/10 in the 2nd cycle to 1C in the 3rd cycle, namely by 10 mAh/g (≡5%) for the pristine NCM-851005 up to 40 mAh/g (≡31%) for the washed NCM-851005 dried at 300°C (see 5th column of Table I).

While the lower initial discharge capacities of the washed/dried NCM-851005 can be rationalized on the basis of a loss of lithium intercalation sites and by an increased cathode impedance of the washed/dried materials, it does not explain the observed strong increase of the capacity fading upon extended cycling with an increase in the drying temperature of the washed NCM-851005 (see last

Table I. Average discharge capacities determined from Figure 10 for the graphite/NCM-851005 full-cells with cathodes based on pristine NCM-851005 or on washed NCM-851005 dried at either 80°C, 180°C, or 300°C. From left to right: discharge capacity of the 2nd C/10 formation cycle (cycle 2 in Figure 10); capacity loss of the washed NCM-851005 cathodes compared to pristine NCM-851005; discharge capacity of the 1st cycle at 1C (cycle 3 in Figure 10); discharge capacity loss when switching from C/10 to 1C (cycles 2 and 3 in Figure 10); discharge capacity loss over 198 cycles at 1C discharge rate (cycles 3 to 200 in Figure 1; charge rate at C/2).

NCM-851005 cath.	2nd C/10 disch. in mAh/g	loss vs. pristine in mAh/g or (%)	1st 1C disch. in mAh/g	loss C/10 → 1C in mAh/g or (%)	loss over 198 1C cycles in mAh/g or (%)
Pristine	188		178	10 (5%)	21 (12%)
washed 2x (80°C)	178	10 (6%)	158	20 (11%)	32 (20%)
washed 2x (180°C)	175	13 (7%)	147	28 (16%)	38 (25%)
washed 2x (300°C)	130	58 (45%)	90	40 (31%)	83 (92%)

column of Table I). The cause of this is found by taking a closer look into the evolution of the voltage vs. capacity profiles, comparing the 3rd cycle with a 1C discharge rate with that of the 28th cycle at 1C for the cathodes with both the pristine NCM-851005 and the washed NCM-851005 dried at 300°C, whose discharge capacity has already dropped by ≈65% at this point. As shown in Figure 10b, the overpotential of the cathode with the pristine NCM-851005, indicated by width of the voltage profiles, as well as the length of the CV phase remain essentially constant between the 1st (solid gray line) and the 25th cycle (dashed gray line) at 1C discharge. This is in stark contrast to the cathode with the washed NCM-851005 dried at 300°C, for which the apparent overpotential as well as the length of the CV phase increase dramatically (black lines). While we unfortunately had not recorded the cathode impedance after the 200 cycles, the evolution of the voltage profiles clearly indicates that the surface layer formed upon

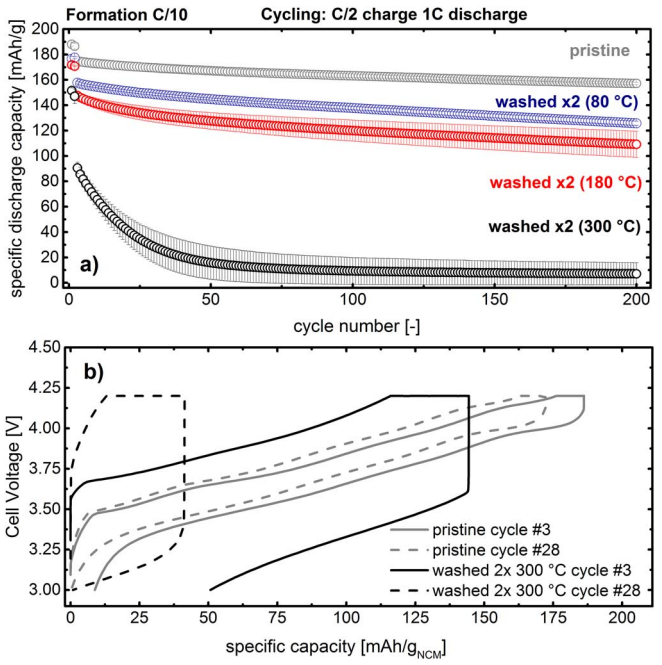

Figure 10. Charge/discharge cycling test of the graphite/NCM-851005 full-cells with a micro-reference electrode shown in Figure 9 and with LP57 electrolyte. After 2 formation cycles at C/10 (shown as the first two cycles), the cycling is carried out with a C/2 charge to 4.2 V (CCCV mode, with a cutoff for the CV phase of C/20) and with a 1C discharge to 3.0 V (CC mode). a) Specific discharge capacities of the pristine NCM-851005 cathode (not washed, dried at 120°C, in gray), and of the washed NCM-851005 cathodes dried at 80°C (in blue), at 180°C (in red), or at 300°C (in black). b) Full-cell voltage vs. capacity profiles of the 3rd and of the 28th cycle at C/2 charge and 1C discharge of the pristine NCM-851005 cathode (in gray) and of the washed NCM-851005 cathode dried at 300°C. The data points represent the average from two measurements and the error bars correspond to the minimum/maximum value of two measurements.

washing/drying according to the here used procedures is unstable and that its impedance increases with extended cycling. Thus, in contrast to the positive effect of washing/drying on the capacity retention of LCO reported by Jeong et al., no such such benefits can be observed for NCM-851005 under the here explored washing/drying conditions.

Conclusions

In this study, we have analyzed the washing process of a nickel-rich cathode active material (NCM 851005) in pure water at room temperature. We showed that Li_2CO_3 surface contaminants are removed by a simple dissolution mechanism, so that it cannot be detected anymore in subsequent washing step if it is conducted in a CO_2-free environment. On the other hand, LiOH is formed continuously during washing due to a near-surface Li^+/H^+ ion exchange, so that the fraction of LiOH ascribable to the dissolution of LiOH surface contaminants cannot be quantified. The washed samples were analyzed by on-line electrochemical mass spectrometry (OEMS) in terms of gassing, revealing that the release of O_2 and CO_2 above 80% SOC decreases substantially as the drying temperature of the washed NCM-851005 is increased from 25°C to 300°C, along with the cathode impedance. With a detailed TGA-MS analysis we could deconvolute the evolution of oxygen and water during the drying process, which is consistent with a near-surface Li^+/H^+ ion exchange during washing and with the formation of a MOOH-like surface structure, which is then thermally decomposed in an oxygen-deficient surface layer. These findings demonstrate that the drying temperature is a critical step when washing Ni-rich NCMs.

Acknowledgment

Financial support by the BASF SE through its Research Network on Electrochemistry and Batteries is gratefully acknowledged.

ORCID

Daniel Pritzl https://orcid.org/0000-0002-9029-107X
Tobias Teufl https://orcid.org/0000-0001-5889-5204
Benjamin Strehle https://orcid.org/0000-0001-8878-1160
Johannes Sicklinger https://orcid.org/0000-0003-2815-993X

References

1. D. Larcher and J. M. Tarascon, *Nat. Chem.*, **7**(1), 19 (2015).
2. D. Andre, S.-J. Kim, P. Lamp, S. F. Lux, F. Maglia, O. Paschos, and B. Stiaszny, *J. Mater. Chem. A*, **3**(13), 6709 (2015).
3. G. E. Blomgren, *J. Electrochem. Soc.*, **164**(1), A5019 (2016).
4. M.-H. Kim, H.-S. Shin, D. Shin, and Y.-K. Sun, *J. Power Sources*, **159**(2), 1328 (2006).
5. P. Rozier and J. M. Tarascon, *J. Electrochem. Soc.*, **162**(14), A2490 (2015).
6. R. Jung, R. Morasch, P. Karayaylali, K. Phillips, F. Maglia, C. Stinner, Y. Shao-Horn, and H. A. Gasteiger, *J. Electrochem. Soc.*, **165**(2), A132 (2018).
7. I. A. Shkrob, J. A. Gilbert, P. J. Phillips, R. Klie, R. T. Haasch, J. Bareño, and D. P. Abraham, *J. Electrochem. Soc.*, **164**(7), A1489 (2017).
8. J. Sicklinger, M. Metzger, H. Beyer, D. Pritzl, and H. A. Gasteiger, *J. Electrochem. Soc.*, **166**(12), A2322 (2019).

9. N. V. Faenza, L. Bruce, Z. W. Lebens-Higgins, I. Plitz, N. Pereira, L. F. J. Piper, and G. G. Amatucci, *J. Electrochem. Soc.*, **164**(14), A3727 (2017).
10. J. Paulsen, H.-K. Park, and Y.-H. Kwon, *US 2009/0224201 A1* (2009).
11. J. Paulsen and J. H. Kim, *WO 2012/107313 A1* (2012).
12. D.-H. Kim and J. Paulsen, *United States Pat. Appl.*, **20160036557**, *WO 2015/128722 A1* (2015).
13. J. Paulsen, H. P. Hong, and H. S. Ahn, *WO 2015/036882 A2* (2015).
14. J. Paulsen, H. P. Hong, and J. D. Oh, *WO 2016/055911 A1* (2016).
15. J. R. Dahn, R. Fong, and U. v. Sacken, *US 2*, *264*, *201* (1993).
16. G. V. Zhuang, G. Chen, J. Shim, X. Song, P. N. Ross, and T. J. Richardson, *J.Power Sources*, **134**(2), 293 (2004).
17. J. Kim, H. Lee, H. Cha, M. Yoon, M. Park, and J. Cho, *Adv. Ener. Mater.*, **8**(6) (2018).
18. Y. Kim, *J. Mater. Sci.*, **48**(24), 8547 (2013).
19. S. E. Renfrew and B. D. McCloskey, *J. Am. Chem. Soc.*, **139**(49), 17853 (2017).
20. R. Jung, P. Strobl, F. Maglia, C. Stinner, and H. A. Gasteiger, *J. Electrochem. Soc.*, **165**(11), A2869 (2018).
21. M. Metzger, B. Strehle, S. Solchenbach, and H. A. Gasteiger, *J. Electrochem. Soc.*, **163**(7), A1219 (2016).
22. H.-J. Noh, S. Youn, C. S. Yoon, and Y.-K. Sun, *J. Power Sources*, **233**, 121 (2013).
23. S. Arimoto, K. Tsuruta, R. Leblanc, R. Melsert, and US 2017/02946521 A1 (2017).
24. J. Kim, Y. Hong, K. S. Ryu, M. G. Kim, and J. Cho, *Electrochem. Solid State Lett.*, **9**, A19 (2006).
25. Y. Kim, *J. Solid State Electrochem.*, **17**(7), 1961 (2013).
26. X. Xiong, Z. Wang, P. Yue, H. Guo, F. Wu, J. Wang, and X. Li, *J. Power Sources*, **222**, 318 (2013).
27. R. Jung, M. Metzger, F. Maglia, C. Stinner, and H. A. Gasteiger, *J. Electrochem. Soc.*, **164**(7), A1361 (2017).
28. D. Streich, C. Erk, A. Guéguen, P. Müller, F.-F. Chesneau, and E. J. Berg, *J. Phys. Chem. C*, **121**(25), 13481 (2017).
29. R. Jung, M. Metzger, F. Maglia, C. Stinner, and H. A. Gasteiger, *J. Phys. Chem. Lett.*, **8**(19), 4820 (2017).
30. T. Teufl, B. Strehle, P. Müller, H. A. Gasteiger, and M. A. Mendez, *J. Electrochem. Soc.*, **165**(11), A2718 (2018).
31. J. Sicklinger, H. Beyer, L. Hartmann, F. Riewald, and H. A. Gasteiger, *mansucript in preparation*.
32. H. Sclar, J. Sicklinger, E. M. Ericson, S. Maiti, J. Grinblat, M. Talianker, L. Burstein, H. Beyer, G. Avruschenko, H. A. Gasteiger, B. Markovsky, and D. Aurbach, *manuscript in preparation*.
33. Z. Chen, J. Wang, J. Huang, T. Fu, G. Sun, S. Lai, R. Zhou, K. Li, and J. Zhao, *J. Power Sources*, **363**, 168 (2017).
34. Y. Cho, S. Lee, Y. Lee, T. Hong, and J. Cho, *Adv. Ener. Mater.*, **1**(5), 821 (2011).
35. Y.-K. Sun, S.-T. Myung, B.-C. Park, J. Prakash, I. Belharouak, and K. Amine, *Nat. Mater.*, **8**, 320 (2009).
36. D. Larcher, M. R. Palacin, G. G. Amatucci, and J. M. Tarascon, *J. Electrochem. Soc.*, **144**, 408 (1997).
37. G. G. Amatucci, J. M. Tarascon, D. Larcher, and L. C. Klein, *Solid State Ionics*, **84**(3), 169 (1996).
38. B. Strehle, K. Kleiner, R. Jung, F. Chesneau, M. Mendez, H. A. Gasteiger, and M. Piana, *J. Electrochem. Soc.*, **164**(2), A400 (2017).
39. N. Tsiouvaras, S. Meini, I. Buchberger, and H. A. Gasteiger, *J. Electrochem. Soc.*, **160**(3), A471 (2013).
40. S. Solchenbach, D. Pritzl, E. J. Y. Kong, J. Landesfeind, and H. A. Gasteiger, *J. Electrochem. Soc.*, **163**(10), A2265 (2016).
41. R. Moshtev, *J. Power Sources*, **81**, 434 (1999).
42. S. Jeong, J. Kim, and J. Mun, *J. Electrochem. Soc.*, **166**(3), A5038 (2019).
43. M. Metzger, C. Marino, J. Sicklinger, D. Haering, and H. A. Gasteiger, *J. Electrochem. Soc.*, **162**(7), A1123 (2015).
44. M. Metzger, B. Strehle, S. Solchenbach, and H. A. Gasteiger, *J. Electrochem. Soc.*, **163**(5), A798 (2016).
45. B. Zhang, M. Metzger, S. Solchenbach, M. Payne, S. Meini, H. A. Gasteiger, A. Garsuch, and B. L. Lucht, *J. Phys. Chem. C*, **119**(21), 11337 (2015).
46. S. Solchenbach, G. Hong, A. T. S. Freiberg, R. Jung, and H. A. Gasteiger, *J. Electrochem. Soc.*, **165**(14), A3304 (2018).
47. J. Wandt, A. T. S. Freiberg, A. Ogrodnik, and H. A. Gasteiger, *Materials Today*, **21**, 218 (2018).
48. K. Luo, M. R. Roberts, R. Hao, N. Guerrini, D. M. Pickup, Y.-S. Liu, K. Edström, J. Guo, A. V. Chadwick, L. C. Duda, and P. G. Bruce, *Nat. Chem.*, **8**, 684 (2016).
49. S. E. Renfrew and B. D. McCloskey, *ACS Appl. Ener. Mater.*, **2**(5), 3762 (2019).
50. S. E. Renfrew, L. A. Kaufman, and B. D. McCloskey, *ACS Appl. Mater. Inter.*, **11**(38), 34913 (2018).
51. A. T. S. Freiberg, M. K. Roos, J. Wandt, R. de Vivie-Riedle, and H. A. Gasteiger, *J. Phys. Chem. A*, **122**(45), 8828 (2018).
52. F. Lin, I. M. Markus, D. Nordlund, T.-C. Weng, M. D. Asta, H. L. Xin, and M. M. Doeff, *Nat. Commun.*, **5**, 3529 (2014).
53. T. Teufl, D. Pritzl, S. Solchenbach, H. A. Gasteiger, and M. A., *J. Electrochem. Soc.*, **166**(6), A1275 (2019).
54. J. Landesfeind, D. Pritzl, and H. A. Gasteiger, *J. Electrochem. Soc.*, **164**(7), A1773 (2017).
55. H. S. Liu, *Electrochem. Solid State Lett.*, **7**(7), A190 (2004).
56. J. Pan, Y. Sun, P. Wan, Z. Wang, and X. Liu, *Electrochem. Commun.*, **7**(8), 857 (2005).
57. S. M. Bak, E. Hu, Y. Zhou, and X. Yu, *ACS Appl. Mater. Inter.*, **6**(24), 22594 (2014).
58. P. G. Bruce, A. R. Armstrong, and R. L. Gitzendanner, *J. Mater. Chem.*, **9**, 193 (1998).
59. M. M. Thackeray, *Prog. Solid State Chem.*, **25**, 1 (1997).
60. S. Solchenbach, M. Metzger, M. Egawa, H. Beyer, and H. A. Gasteiger, *J. Electrochem. Soc.*, **165**(13), A3022 (2018).